Fabrication of Hollow Poly(lactic acid) Microcapsules from Microbubble Templates

ARTICLE *in* THE JOURNAL OF PHYSICAL CHEMISTRY B · NOVEMBER 2009

Impact Factor: 3.3 · DOI: 10.1021/jp9053956 · Source: PubMed

Fabrication of Hollow Poly(lactic acid) Microcapsules from Microbubble Templates

Hirofumi Daiguji,*,† Shingo Takada,† Jay J. Molino Cornejo,† and Fumio Takemura‡

Institute of Environmental Studies, Graduate School of Frontier Sciences, The University of Tokyo, Kashiwa 277-8563, and National Institute of Advanced Industrial Science and Technology (AIST), Tsukuba 305-8564, Japan

Received: June 9, 2009; Revised Manuscript Received: August 24, 2009

Hollow microcapsules are expected to be integral components of drug delivery systems in medical and pharmaceutical applications. Among the methods studied, the bubble template method (Makuta et al. *Mater. Lett.* **2009**, *63*, 703−705) should easily fabricate uniform hollow microcapsules covered with biodegradable polymers. In this study, we clarified the two conditions required to fabricate uniform hollow microcapsules using the bubble template method: the stability of uniformly sized microbubbles in a liquid droplet and the release of hollow microcapsules from the droplet. Furthermore, our experiments evaluated the radius distributions of template microbubbles and fabricated hollow poly(lactic acid) microcapsules.

1. Introduction

Hollow microcapsules of biodegradable polymers with diameter less than 10 μm are expected to be used as ultrasound contrast agents or carriers for drug delivery systems (DDSs) in medical or pharmaceutical applications.[2−6] Hollow microcapsules are generally fabricated as follows.[7] First, solid particles or liquid droplets are dispersed in a continuous gas or liquid phase. Then shell materials are added to the dispersed cores or to the continuous phase. By controlling the temperature, pH, and/or pressure in the continuous phase, shells are formed around each dispersed core by supersaturating the concentration of the shell materials. Shells are also formed by adsorption or reaction of the shell materials onto the surface of the cores. Finally, the permeability and strength of the shell are intentionally degraded by aging or cross-linking so that the liquid or solid core can be removed by dissolution, evaporation, or thermolysis, thus yielding hollow capsules. Several other fabrication methods have been proposed to produce hollow microcapsules for the shell materials of SiO_2, TiO_2, and amino resin.[8−11]

The direct encapsulation of microbubbles with shell materials is another method of fabricating hollow microcapsules. In medical and pharmaceutical applications, stabilized microbubbles covered with a lipid bilayer are expected to be used as ultrasound contrast agents or carriers in DDS.[12,13] With moisture-curing resin, microbubbles can also be directly covered with a polymer film using a polymerization reaction at the bubble surface. For both types of covering (i.e., a lipid bilayer or polymer film), hollow structures can be fabricated using bubbles as templates.[14−17] Such shells, however, easily disintegrate because the interaction between lipid molecules is weak for bubbles covered with a lipid bilayer or because the shell for bubbles covered with a polymer film is too thin. Hollow microcapsules would be suitable for many applications if researchers could find ways to fabricate thicker shells. Recently hollow polyelectrolyte microcapsules were fabricated by layer-by-layer deposition of oppositely charged polyelectrolyte around microbubble templates. It is said that polyelectrolyte multilayers are effective barriers or drastically decrease gas diffusion, but this fabrication method can be used only for polyelectrolyte microcapsules.[18]

For hollow microcapsules used in medical and pharmaceutical applications, biodegradable polymers that can be disintegrated using microbes or bacteria would make the best shell materials. Examples of such polymers include poly(lactic acid) (PLA), poly(glycolic acid), and poly(ε-caprolactone).[19] Because of its slow disintegration rate, PLA is often used for suture thread inside the human body.[20] Moreover, porous microcapsules of these biodegradable polymers made by using a spray-drying method are being developed as an ultrasound perfusion contrast agent[21] and are currently in a clinical trial.[22] The structure of these microcapsules is not a single bubble covered with a biodegradable shell but a porous biodegradable particle that includes multiple internal voids of perfluorocarbon gas. Biodegradable polymers are synthesized from crude materials via a complex multistep fabrication that includes evaporation, distillation, and polymerization.[23] Therefore, it is difficult to encapsulate microbubbles with a biodegradable polymer using a direct polycondensation reaction because microbubbles cannot stay in the liquid during the polycondensation reaction time because of dissolution and bursting. Hollow microcapsules with a biodegradable polymer shell are usually produced by a solvent evaporation method.[24] A conventional solvent evaporation method includes many processes: generation of a water/oil/water (W/O/W) emulsion by sonication, evaporation of the solvent, and freeze-drying for removing the core. More recently, microfluidic devices have been used to make massive numbers of bubbles[25,26] and, in some cases, bubbles coated with polymers.[27] This fabrication method is also categorized into the solvent extraction/evaporation methods. The size of hollow capsules can be controlled by the dimension of microchannels, physical properties of liquids, and flow rate of liquids. However, in this method, smaller microchannels are required for smaller hollow capsules; thus, it is more difficult to fabricate smaller hollow capsules.

To fabricate hollow microcapsules covered with the thick shell of a biodegradable polymer, we developed a simple fabrication method of hollow microcapsules covered with PLA

* To whom correspondence should be addressed. E-mail: daiguji@k.u-tokyo.ac.jp. Phone: +81 4 7136 4658. Fax: +81 4 7136 4659.
† The University of Tokyo.
‡ AIST.

10.1021/jp9053956 CCC: $40.75
Published on Web 10/21/2009

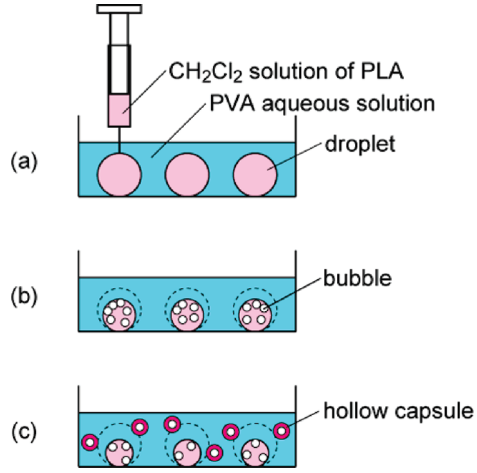

Figure 1. Fabrication procedures of hollow PLA microcapsules in the bubble template method:[1] (a) formation of droplets, (b) generation of microbubbles, (c) release of hollow microcapsules.

by using microbubbles as templates (bubble template method).[1] The bubble template method includes the following three steps as shown in Figure 1.

(1) We prepared a 2 g/L methylene chloride solution of PLA and a 2% (w/w) poly(vinyl alcohol) (PVA) aqueous solution. The droplets of the methylene chloride solution of PLA (about 0.05−0.5 mm in radius) were dispersed in the PVA aqueous solution through a microsyringe. Because of the surface-active properties of PVA, the droplets did not coalesce in the aqueous solution.

(2) We enclosed the droplets and solution in a vessel that was pressurized by air to more than 300 kPa. The air was fully dissolved into both the droplets and solution. Then we decreased the pressure of the vessel to atmospheric pressure, thus yielding microbubbles in the droplets as well as in the solution because of degassing. Microbubbles in the droplets had a uniform radius and remained stable, whereas those in the solution soon disappeared.

(3) As the droplet shrank due to the dissolution of methylene chloride into the PVA aqueous solution, hollow PLA microcapsules, whose inner radius was the same as that of the bubbles, released spontaneously from the droplet into the PVA aqueous solution.

This fabrication method can also be categorized into the solvent extraction/evaporation methods. After degassing, nucleation of bubbles, physisorption of PLA onto microbubbles, extraction of hollow PLA microcapsules into the PVA aqueous solution, and solvent evaporation take place sequentially as the droplet shrinks. One of the advantages in the bubble template method is that all these processes take place spontaneously without application of any external forces. Two important processes in the bubble template method are the preparation of uniformly sized microbubbles as templates, as shown in Figure 1b, and the encapsulation of microbubbles and the release from the droplet, as shown in Figure 1c. For the preparation of uniformly sized microbubbles, we focused on the phenomenon through which bubbles in a closed volume of liquid−gas solution have a uniform radius and can be thermodynamically stable. It is critical to control precisely the bubbles' radius for the development of a uniformly sized hollow microcapsule. In the bulk liquid, some microbubbles coalesce into large bubbles and float into the air, and others disappear due to the dissolution of the gases into the liquid. In contrast, in a closed volume of liquid−gas solution, the bubble radius must be the same in the equilibrium state because the equilibrium radius, r, is determined by $2\gamma/p$, where p is the vapor pressure of the liquid, which is close to the saturation vapor pressure of the pure liquid, and γ is the surface tension. Ward et al.[28] reported the stability of bubbles in a closed volume of liquid−gas solution, but the stability conditions have not yet been clarified. For the encapsulation process, we succeeded in fabricating hollow PLA microcapsules without applying any external forces. However, microbubbles covered with PLA did not always move away from the droplets into the PVA aqueous solution. The conditions for the release of hollow PLA microcapsules have not yet been clarified.

The objective of this study was to clarify the following two conditions: (1) conditions required for the stability of uniformly sized microbubbles inside a droplet of methylene chloride solution of PLA and (2) conditions required for the release of hollow PLA microcapsules from the droplet. Furthermore, our experiments evaluated the radius distributions of template microbubbles and fabricated hollow PLA microcapsules.

2. Theory

2.1. Conditions Required for the Stability of Uniformly Sized Microbubbles inside a Droplet. The first step to fabricate uniformly sized hollow microcapsules is to maintain uniformly sized template bubbles in a liquid long enough to form a capsule shell. Ward et al.[28] reported that bubbles in a closed volume of liquid−gas solution can be thermodynamically stable. The observed system was not completely closed because methylene chloride transferred to the surrounding PVA aqueous solution. However, the dissolution rate of methylene chloride into the PVA aqueous solution was much slower than the relaxation rate needed to achieve the liquid−vapor equilibrium. Furthermore, air bubbles were generated due to the dissolution of methylene chloride because the solubility of arbitrary gas in aqueous solution[29] was generally much smaller than that in methylene chloride.[30] However, the generation rate of microbubbles was also much slower than the relaxation rate needed to achieve the liquid−vapor equilibrium. Therefore, the observed system could be regarded as a closed system. According to the analysis of Ward et al.,[28] the differential of the total potential B of a closed system of liquid−gas solution for the virtual displacement in the equilibrium state can be expressed as

$$\delta B = q(-p'' + p')\,\delta V'' + q\gamma\,\delta S + \mu_1''\,\delta N_1'' + \mu_1'\,\delta N_1' + \mu_2''\,\delta N_2'' + \mu_2'\,\delta N_2' \quad (\text{at } p', T, N_1, \text{and } N_2 = \text{constant}) \quad (1)$$

where q, p, V, S, N, γ, μ, and T are the total number of bubbles, the pressure, volume, and surface area of a bubble, the number of moles, the surface tension, the chemical potential, and the temperature, respectively. The subscripts 1 and 2 denote a volatile liquid (methylene chloride) and a noncondensable gas (air), and single and double primes refer to the liquid and gas phases, respectively; p and V without subscripts and N_1 and N_2 without single/double primes denote the summation of each component and each phase, respectively. Considering the virtual displacement of the spherical bubble radius, r, eq 1 yields

$$\frac{dB}{dr} = 4\pi q r^2\left(-p'' + p' + \frac{2\gamma}{r}\right) + q(\mu_1'' - \mu_1')\frac{dN_1''}{dr} + q(\mu_2'' - \mu_2')\frac{dN_2''}{dr} \quad (2)$$

In the equilibrium state, the following relationships, that is, the equity of chemical potential and the Laplace relation, are satisfied:

$$\mu_i'' = \mu_i' \quad (\text{for } i = 1 \text{ or } 2) \tag{3}$$

$$p'' = p' + \frac{2\gamma}{r} \tag{4}$$

From eqs 3 and 4, $dB/dr = 0$ in the equilibrium state. Furthermore, it was assumed that the derivative of eq 4 is also satisfied:

$$\frac{dp''}{dr} = -\frac{2\gamma}{r^2} \tag{5}$$

From eqs 3−5, the second derivative of B with respect to r is expressed as follows:

$$\frac{d^2B}{dr^2} = q\left(\frac{d\mu_1''}{dr} - \frac{d\mu_1'}{dr}\right)\frac{dN_1''}{dr} + q\left(\frac{d\mu_2''}{dr} - \frac{d\mu_2'}{dr}\right)\frac{dN_2''}{dr} \tag{6}$$

If it is assumed that the gas and liquid components form a weak solution in the liquid phase and an ideal mixture in the gaseous phase, eq 6 yields

$$\frac{d^2B}{dr^2} = \frac{4\pi q r^3}{3p_1''}\left(\frac{dp_1''}{dr} + \frac{p_1''}{K_H}\frac{dp_2''}{dr}\right)\left(\frac{3p_1''}{r} + \frac{dp_1''}{dr}\right)$$

$$= \frac{4\pi q r^3}{3p_1''}\left[\left(1 - \frac{p_1''}{K_H}\right)\frac{dp_1''}{dr} - \frac{p_1''}{K_H}\frac{2\gamma}{r^2}\right]\left(\frac{3p_1''}{r} + \frac{dp_1''}{dr}\right) \tag{7}$$

where K_H is Henry's law constant (see the Appendix, section A.1). For a weak solution, p_1''/K_H is negligible compared to unity. If the vapor pressure of a volatile liquid is independent of r, i.e., $dp_1''/dr = 0$, the system is unstable, i.e., $d^2B/dr^2 < 0$. This is the case in open systems where bubbles are in the bulk liquid instead of a liquid droplet. In contrast, in closed systems, because the total numbers of moles, N_1 and N_2, are constant, dp_1''/dr is nonzero and controlled by adjusting the dissolved gas concentration, c_2'. From eq 7, the condition for stability can be expressed as follows (see the Appendix, section A.2):

$$q > \frac{3c_{01}V'RT}{4\pi r^3 K_H}\left[\left(\frac{K_H}{p_1''} + \frac{p_1''}{K_H} - 2\right)\frac{3p_1''p_2''r}{2\gamma K_H} - \left(\frac{K_H}{p_2''} + \frac{p_1''}{K_H}\right)\frac{p_2''}{K_H}\right]^{-1}$$

$$q > \frac{3c_{01}V'RT}{4\pi r^3 K_H}\left[\frac{3p_2''r}{2\gamma} - 1\right]^{-1} \equiv q_0 \quad \left(\text{at } \frac{p_1''}{K_H} \ll 1\right) \tag{8}$$

This relationship indicates that the system becomes stable when q is larger than the threshold number of q_0. When the stability condition (eq 8) is satisfied and the concentration of air in the liquid phase achieves the saturation concentration, eq 4 becomes $p_1'' = 2\gamma/r$ and $p_2'' = p'$. If p_1'' is approximated to the saturation vapor pressure of pure liquid, p_{01}'', the equilibrium radius of bubbles becomes

$$r_{eq} = 2\gamma/p_{01}'' \tag{9}$$

2.2. Conditions Required for the Release of Hollow PLA Microcapsules from a Droplet. In the bubble template method,[1] microbubbles were stable in the droplet of the methylene chloride solution of PLA, as shown in Figure 1b. However, microbubbles coalesced or disappeared in the droplet without PLA. This result suggests that PLA adsorbs to the surface of microbubbles because of its surface-active property. Sequentially, microbubbles covered with PLA were released from the droplet to the surrounding PVA aqueous solution, as shown in Figure 1c. The droplet shrank due to the dissolution of methylene chloride into the PVA aqueous solution, and the PLA concentration increased. However, the release of microcapsules stopped before complete dissolution of methylene chloride into the surrounding PVA aqueous solution.

In this study, we focused on the concentration of PLA in the methylene chloride solution, c_3, as a parameter to identify the start and stop times for the release of hollow PLA microcapsules from the droplet. By assuming that the total volume of bubbles in comparison to the total volume of a droplet, V_d, is negligible, and a part of PLA adsorbs onto the bubbles and capsules, the mass conservation equation of PLA can be expressed as follows:

$$c_3V_d = c_{30}V_{d0} - \Gamma_{bc}^{eq}(c_3)\sum S_{bc} \tag{10}$$

where c_{30} and V_{d0} are the initial values of c_3 and V_d, $\Gamma_{bc}^{eq}(c_3)$ is the equilibrium area density of PLA on the surface of the bubbles and capsules at c_3, and $\sum S_{bc}$ is the total surface area of the bubbles and capsules. Here, the relationship between c_3 and V_d was modeled by assuming that the release of hollow PLA microcapsules started at c_{3min} and stopped at c_{3max}, where c_{3min} is a threshold value of c_3 at which PLA adsorbs on the surface of the bubbles so much that the bubbles can remain stable and c_{3max} is the solubility of PLA in methylene chloride. For simplicity, the bubbles are unstable, that is, $\sum S_{bc} = 0$, at $c_3 < c_{3min}$, whereas the bubbles are stable and PLA is fully adsorbed on the surface of the bubbles and capsules, that is, $\Gamma_{bc}^{eq}(c_3)$ is a constant value of Γ_{bc}^{max}, at $c_3 \geq c_{3min}$. Specifically

$$c_3V_d = c_{30}V_{d0} \quad \text{at} \quad c_3 < c_{3min} \tag{11}$$

$$c_3V_d = c_{30}V_{d0} - \Gamma_{bc}^{max}\sum S_{bc} \quad \text{at} \quad c_3 \geq c_{3min} \tag{12}$$

At $c_3 \geq c_{3min}$, if all bubbles and capsules have an equilibrium radius, r_{eq}, $\sum S_{bc}$ is given by the following equation:

$$\sum S_{bc} = \frac{3}{r_{eq}}\sum V_{bc} \tag{13}$$

where $\sum V_{bc}$ is the total volume of bubbles and capsules. Here, the following two assumptions were employed: (1) As the droplet shrinks, air dissolving in the solution forms bubbles because the solubility of air in the solution is much higher than that in the PVA aqueous solution. (2) When the generated bubbles arrive at the interface between the droplet and the surrounding PVA aqueous solution, a part of the bubbles stay, and others collapse at the interface. Because the diffusion rate of PLA is much slower than the flow rate of the bubbles, the average area density of PLA at the surface of the bubbles, $\bar{\Gamma}_{bc}$, is smaller than Γ_{bc}^{max} just when the bubbles arrive at the interface.

If the diffusion of PLA is negligible, $\bar{\Gamma}_{bc}$ is given by $\Gamma_{bc} = c_3\bar{d}A_{bc}/S_{bc}$, where $\bar{d}$ is the average traveling distance of the bubbles, which is proportional to the radius of a droplet, r_d ($\bar{d} = \delta r_d$), and A_{bc} is the collision cross section. Here, the survival ratio of bubbles at the interface, R_s, is assumed to be proportional to $\bar{\Gamma}_{bc}/\Gamma_{bc}^{max}$ ($R_s = \varepsilon\bar{\Gamma}_{bc}/\Gamma_{bc}^{max}$). From these two assumptions, the derivative of $\sum V_{bc}$ with respect to time can be expressed as follows:

$$\frac{d}{dt}\left(\sum V_{bc}\right) = -\alpha\frac{dV_d}{dt}R_s \tag{14}$$

where α is the ratio between the saturation concentration of air in the methylene chloride solution and air density in the gas phase, that is, $\alpha = c_{2s}RT/p_2''$. From eqs 13 and 14, eq 12 becomes

$$c_3V_d = c_{30}V_{d0} + \frac{\alpha\beta}{r_{eq}}\int\frac{dr_d}{dt}c_3V_d\,dt \tag{15}$$

where $\beta = \delta\varepsilon A_{bc}/S_{bc}$. If dr_d/dt is constant, eq 15 can be simplified as follows:

$$\frac{d}{dt}(c_3V_d) = \kappa(c_3V_d) \tag{16}$$

where $\kappa = (\alpha\beta/r_{eq})(dr_d/dt)$. The condition for constant dr_d/dt is explained in the Appendix, section A.3. By solving eq 16, the total mass of PLA in the bulk solution, c_3V_d, is given by

$$c_3V_d = c_{30}V_{d0}\exp(\kappa t) \tag{17}$$

By employing the above assumptions, eq 12 was transformed into eq 17. In summary, if $c_{30} < c_{3min}$, the release of hollow PLA capsules starts at c_{3min} and stops at c_{3max}. From eqs 11 and 17, the release of capsules starts at the droplet size of $V_d = (c_{30}/c_{3min})V_{d0}$ and stops at $V_d = (c_{30}/c_{3max})V_{d0}\exp(\kappa t)$.

3. Experiment

3.1. Chemicals. The shell material was PLA with a molecular weight of 2000 (PolyScience, Niles, IL). Methylene chloride (Wako Pure Chemical Industries, Ltd., Osaka, Japan) was used for the PLA solution. The continuous phase was 2% (w/w) PVA aqueous solution made from anionic poly(vinyl alcohol) (the typical degree of polymerization is 1800) (Gohsenal T-350, Nippon Gohsei, Osaka, Japan). All chemicals used in this study were reagent grade.

3.2. Methods. The methods of fabricating hollow PLA microcapsules were the same as those used in our previous study and discussed in section 1 except for the bubble generation process (also see Figure 1). In the previous study, microbubbles were generated by applying air pressure and degassing, whereas, in this study, microbubbles were generated without application of air pressure. Because the initial concentration of dissolving air in a methylene chloride solution of PLA was close to the saturation concentration and the solubility of air in a PVA aqueous solution was much smaller than that in a methylene chloride solution of PLA, microbubbles were generated due to the dissolution of methylene chloride into the surrounding PVA aqueous solution without application of air pressure. The radius distribution of the bubbles was obtained by processing several bright field images of the bubbles in several focused planes inside a droplet using an inverted microscope system (ECLIPSE Ti-E, Nikon Corp., Tokyo, Japan). The generated hollow PLA microcapsules were purified, dried, and then observed. Because PLA was stained with Nile Red, hollow PLA microcapsules were visualized as fluorescence images. The inner and outer radius distributions of the hollow PLA capsules were obtained by processing several bright field images of capsules.

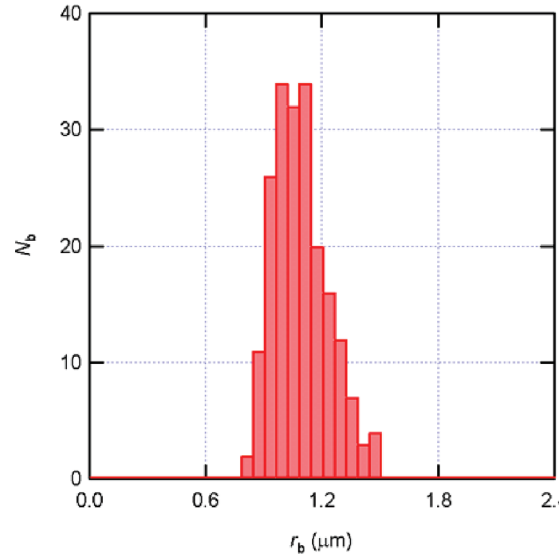

Figure 2. Number of bubbles, N_b, vs radius, r_b, histogram.

To verify the conditions for the release of hollow PLA microcapsules from a droplet, a 500 μm radius droplet of the methylene chloride solution of PLA with five different initial concentrations of PLA—c_{30} = 20, 2, 0.2, 0.02, and 0.002 g/L—was formed inside a 2% (w/w) PVA aqueous solution by using a microsyringe, and the shrinkage of the droplet and the release of hollow PLA capsules were recorded as a movie. The time evolution of the droplet radius of methylene chloride solutions of PLA, r_d, and the start and stop times for the release of hollow PLA microcapsules were obtained by analyzing the movie. In this experiment, microbubbles were also generated without application of air pressure. All the experiments were executed at 298 K.

4. Results and Discussion

Figure 2 shows the frequency histogram of the bubble radius, r_b. The mean radius and the standard deviation were 1.03 and 0.14 μm, respectively. The polydispersivity index (PI = standard deviation/mean) values for the bubbles was 13.6%. By substituting $\gamma = 2.78 \times 10^{-2}$ N/m[31] and $p_{01}'' = 5.81 \times 10^4$ Pa[32] at 298 0.15 K into eq 10, r_{eq} was calculated as 0.95 μm. The measured bubble radius agreed with the theoretical prediction.

Figure 3 shows the time evolution of the droplet radius of methylene chloride solutions of PLA, r_d, for five different c_{30} values. On the x axis, time was set as $t = 0$ at $r_d = 0.42$ mm. Except for the region at $t > 45$ min, r_d decreased almost linearly with respect to t. The line fitted to all the data except for c_{30} = 20 g/L within the range of $0 \le t \le 45$ min was r_d (mm) = 0.42 − 0.0065[t (min)]. If the dissolution rate of methylene chloride into the surrounding PVA aqueous solution is restricted by the surface area of a droplet and is not restricted by the diffusion in the PVA aqueous solution, dr_d/dt remains constant (see the Appendix, section A.3). This experimental result confirmed the validity of the transformation of eq 15 into eq 16. Furthermore, at $t > 20$ min, $|dr_d/dt|$ of c_{30} = 20 g/L was smaller than that of

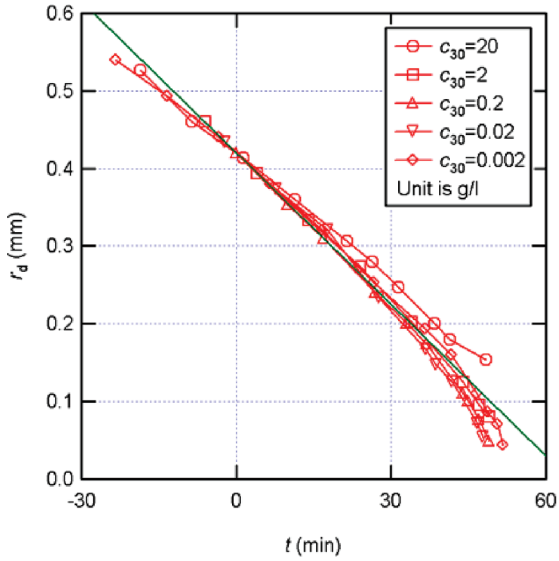

Figure 3. Time evolution of the droplet radius of methylene chloride solutions of PLA, r_d, for five different initial concentrations of PLA, c_{30}. Time (x axis) was set as $t = 0$ at $r_d = 0.42$ mm. The line fitted to all the data except for $c_{30} = 20$ g/L within the range of $0 \le t \le 45$ min was r_d (mm) $= 0.42 - 0.0065[t$ (min)].

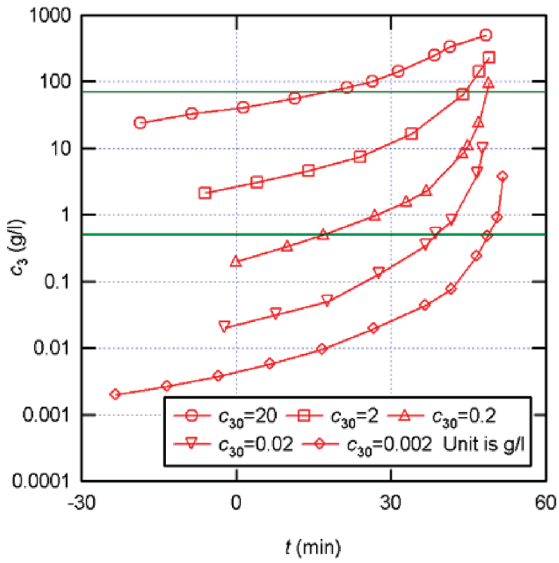

Figure 4. Time evolution of the concentration of methylene chloride solutions of PLA, c_3, for five different initial concentrations of PLA, c_{30}. Time (x axis) was set as $t = 0$ at $r_d = 0.42$ mm. The lines show $c_3 = 0.5$ and 70 g/L. Hollow PLA microcapsules released from a droplet within the range of 0.5 g/L $\le c_3 \le$ 70 g/L.

the other c_{30} values. This experimental result suggested that c_3 increased beyond the solubility around $t = 20$ min for $c_{30} = 20$ g/L, and the diffusion of methylene chloride inside the droplet could restrict the overall dissolution rate. For $c_{30} = 20$ and 2 g/L, the release of hollow PLA microcapsules started just after the formation of a droplet and stopped at $t = 20$ and 44 min, respectively. For these two c_{30} values, the fluidity of a droplet was not lost when the release of hollow PLA microcapsules stopped. However, for $c_{30} = 0.2$, 0.02, and 0.002 g/L, hollow PLA microcapsules did not release just after the formation of a droplet. The release of hollow PLA microcapsules started at $t = 17$, 39, and 49 min, respectively, and stopped when a droplet became a solid particle.

Figure 4 shows the time evolution of c_3 for five different c_{30} values that was calculated from eqs 11 and 17. On the x axis, time was also set as $t = 0$ at $r_d = 0.42$ mm. The threshold value of c_{3min} was determined from eq 11 by using c_{30}, V_{d0}, and the volume of a droplet when the capsule release started. The calculated c_{3min} values were 0.50, 0.52, and 0.48 g/L for $c_{30} = 0.2$, 0.02, and 0.002 g/L, respectively. Therefore, the threshold value of c_{3min} could be determined to be about 0.5 g/L. At $c_3 < c_{3min}$, c_3 was calculated from eq 11, whereas, at $c_3 \ge c_{3\,min}$, c_3 was calculated from eq 17 by assuming $\kappa = -0.01$ min^{-1}. Assuming that $r_{eq} = 0.95$ μm, $dr_d/dt = -6.5$ μm/min (from Figure 3), and $\alpha = c_{2s}RT/p_2'' \approx 0.5$, the parameter κ $(=(\alpha\beta/r_{eq})(dr_d/dt))$ is given by $\kappa = -3.4\beta$ min^{-1}. The parameter β $(=\delta\varepsilon A_{bc}/S_{bc})$ consists of three parameters, δ, ε, and A_{bc}/S_{bc}, and the last parameter A_{bc}/S_{bc} can be approximated with $A_{bc}/S_{bc} = \pi r_{eq}^2/4\pi r_{eq}^2 = 0.25$. It is difficult to make models to identify these parameters δ and ε, but if it is assumed that $\delta = 1$ and $\varepsilon = 0.01$, i.e., $\bar{d} = r_d$ and 1% of PLA fully adsorbed bubbles survive, $\kappa = -0.01$ min^{-1} but each parameter should be close to unity. Thus, the order of parameter κ was estimated to be 0.01. The solubility of c_{3max} was determined from eq 17 by using c_{30}, V_{d0}, and the volume of a droplet when the capsule release stopped. The calculated c_{3max} values were 82 and 64 for $c_{30} = 20$ and 2 g/L, respectively. Because the measured solubility of PLA in methylene chloride was 70 g/L at room temperature, the calculated c_{3max} was close to the solubility. By using the theoretical model shown in the previous section, the experimental results could be reasonably explained if the release of hollow PLA microcapsules started at $c_3 = 0.5$ g/L and stopped at 70 g/L independent of the initial concentration of PLA and initial radius of a droplet.

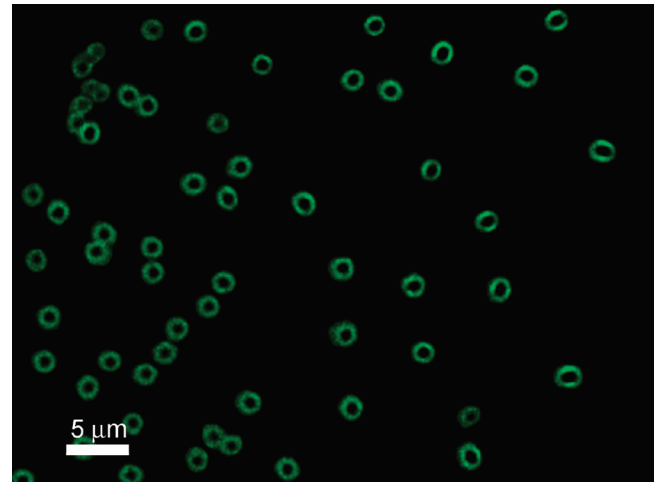

Figure 5. Epifluorescence image of hollow PLA microcapsules.

Figure 5 shows the epifluorescence image of hollow PLA microcapsules. PLA was stained with Nile Red, and the excitation wavelength was 552 nm. Figure 5 shows low-fluorescence-intensity rings with a dark area inside the spheres, clearly indicating that fabricated microspheres were hollow microcapsules with a single internal void. Figure 6 shows the number of hollow PLA capsules, N_c, vs either inner radius, r_{ci}, or outer radius, r_{co}, histogram. The average inner radius was 0.41 μm, and the standard deviation was 0.04 μm (PI = 10%). The average outer radius was 1.03 μm, and the standard deviation was 0.08 μm (PI = 7.7%). The shell thickness calculated from the difference between the average inner and outer radii was 0.62 μm. Because the mean value of the template bubble radius was about 1.03 μm, the inner radius of the capsules was smaller than that of the template bubbles. This experimental result suggested that hollow PLA capsules shrank before the shell was solidified. The possible reasons for the

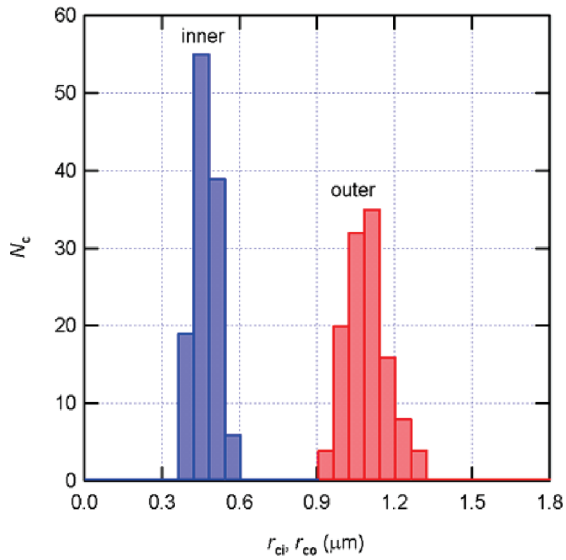

Figure 6. Number of hollow PLA capsules, N_c, vs either inner radius, r_{ci}, or outer radius, r_{co}, histogram.

shrinkage are as follows: (1) Inside a methylene chloride droplet, the gas inside the bubbles is a mixture of methylene chloride and air. After being released into a PVA aqueous solution, most of the methylene chloride gas could dissolve into the PVA aqueous solution. (2) In the vicinity of a methylene chloride droplet, the concentration of methylene chloride in a PVA aqueous solution is so high that a part of the air could also dissolve into the PVA aqueous solution. (3) During solvent evaporation, the molecular distance between PLA molecules is shortened and the intermolecular interaction gets stronger, and this excerts pressure on the inner gas, forcing it to the outside of the capsule until the capsule completely solidifies. The modeling of the solvent evaporation process after release into the PVA aqueous solution is an ongoing study. The successful control of the shrinkage enables the bubble template method to be more controllable.

5. Conclusions

Two important processes in the bubble template method are the preparation of uniformly sized microbubbles as templates and the encapsulation of microbubbles and the release from the droplet. About these two processes, the following conclusions could be drawn from both the theoretical and experimental studies:

(1) In the theoretical analysis, when determining the condition for the stability of uniformly sized microbubbles inside a droplet, we concluded that the number of bubbles, q, was larger than the threshold number of q_0 (eq 8). When the stability condition was satisfied and the concentration of air in the liquid phase achieved the saturation concentration, the equilibrium radius of the bubbles was approximated with $r_{eq} = 2\gamma/p_{01}''$ (eq 9), where p_{01}'' is the saturation vapor pressure of the pure liquid and γ is the surface tension. The mean value of the measured bubble radius was 1.03 μm and agreed with the theoretical prediction of 0.95 μm.

(2) The relationship between the concentration of PLA, c_3, and the volume of a droplet, V_d, was modeled by assuming that the release of hollow PLA microcapsules started at c_{3min} and stopped at c_{3max}, where c_{3min} is the threshold value of c_3 at which PLA adsorbed on the surface of the bubbles so much that the bubbles remained stable and c_{3max} is the solubility of PLA in methylene chloride. By using this model, the experimental results could be reasonably explained if the release of hollow PLA microcapsules started at $c_{3min} = 0.5$ g/L and stopped at $c_{3max} = 70$ g/L, independent of the initial concentration of PLA and initial radius of a droplet.

(3) The average inner and outer radii of hollow PLA microcapsules were 0.41 and 1.03 μm, respectively. The average shell thickness was 0.62 μm. The average inner radius was smaller than that of the template bubbles, suggesting that hollow PLA capsules shrank before the shell was solidified.

Acknowledgment. This research was supported by a Grant-in-Aid for Scientific Research (B) (No. 20360093) from the Japan Society for the Promotion of Science (JSPS).

Appendix

A.1. Second Derivative of B with Respect to r for a Weak Solution

If it is assumed that the gas and liquid components form a weak solution in the liquid phase and an ideal mixture in the gaseous phase, then the explicit expressions for the chemical potentials are as follows:

$$\mu_1'' = v_0 p_{01}'' + RT \ln\left(\frac{p_1''}{p_{01}''}\right) \tag{a1}$$

$$\mu_2'' = \mu_{20}'' + RT \ln\left(\frac{p_2''}{p'}\right) \tag{a2}$$

$$\mu_1' = v_0 p' + RT \ln\left(\frac{c_2'}{c_1' + c_2'}\right) = v_0 p' - RT \ln\left(1 + \frac{c_2'}{c_1'}\right) \approx v_0 p' - RT\left(\frac{c_2'}{c_1'}\right) \quad \text{at} \quad c_2' \ll c_1' \tag{a3}$$

$$\mu_2' = \mu_{20}' + RT \ln\left(\frac{c_2'}{c_{2s}}\right) \tag{a4}$$

where R and T are the gas constant and temperature, respectively. v_0, p_{01}'', and c_{2s} are the specific volume of the pure liquid, the saturation pressure of the pure liquid, and the saturation concentration of the gas in the liquid phase, respectively. μ_{20}'' and μ_{20}' are the chemical potentials of the gas in the gaseous and liquid phases when the gas is dissolved up to the saturation concentration ($p_2'' = p'$ and $c_2' = c_{2s}$). Assuming that $c_1' \equiv N_1'/V' = c_{01}$, the variables are only p_1'', p_2'', and c_2'. The derivatives of eqs a1−a4 with respect to the bubble radius lead to the following equations:

$$\frac{d\mu_2''}{dr} = \frac{d\mu_2'}{dr} = \frac{RT}{p_2''}\frac{dp_2''}{dr} \tag{a5}$$

$$\frac{d\mu_1''}{dr} = \frac{RT}{p_1''}\frac{dp_1''}{dr} \tag{a6}$$

$$\frac{d\mu_1'}{dr} = -\frac{RT}{c_{01}}\frac{dc_2'}{dr} = -\frac{RT}{K_H}\frac{dp_2''}{dr} \tag{a7}$$

where Henry's law was assumed, namely

$$p_2'' = K_H \frac{c_2'}{c_{01}} \tag{a8}$$

where K_H is Henry's law constant. Substituting eqs a5−a7 and $N_1'' = 4\pi r^3 p_1''/3RT$ into eq 6, eq 6 yields eq 7.

A.2. Transformation of the Stability Condition

The total number of moles of a volatile liquid and a noncondensable gas can be written as

$$N_1 = c_{01}V' + qN_1'' \tag{a9}$$

$$N_2 = c_2'V' + qN_2'' \tag{a10}$$

At fixed N_1 and N_2, the derivatives of eqs a9 and a10 are transformed as the following equations by assuming the derivatives of the ideal gas equation and Henry's law (eq a8):

$$\frac{dp_1''}{dr} = -\left(\frac{RT}{V''}\frac{c_{01}}{q}\frac{dV'}{dr} + \frac{3p_1''}{r}\right) \tag{a11}$$

$$\frac{dp_2''}{dr} = -\frac{1}{x}\left(\frac{RT}{V''}\frac{c_2'}{q}\frac{dV'}{dr} + \frac{3p_2''}{r}\right) \tag{a12}$$

where $x = 1 + c_2'V''RT/qp_2''V'' \equiv 1 + N_2'/qN_2''$. Substituting eqs a11 and a12 into eq 5, dV'/dr is given by

$$\frac{dV'}{dr} = -\frac{3qp_1''V''}{c_{01}RTr}\frac{(1 - 2\gamma/3p_1''r)x + (p_2''/p_1'')}{x + (c_2'/c_{01})} \tag{a13}$$

From eq 7, the condition for stability can be expressed as follows:

$$\frac{dp_1''}{dr} + \frac{p_1''}{K_H}\frac{dp_2''}{dr} > 0 \tag{a14}$$

From eqs a11-a13, the stability condition in eq a14 can be transformed as follows:

$$\frac{dp_1''}{dr} + \frac{p_1''}{K_H}\frac{dp_2''}{dr} = \frac{3p_1''}{r}\left[\frac{x + (p_1''/K_H)(c_2'/c_{01})}{x + (c_2'/c_{01})}\left\{\left(1 - \frac{2\gamma}{3p_1''r}\right)x + \frac{p_2''}{p_1''}\right\} - \left(x + \frac{c_2'}{c_{01}}\right)\right] > 0 \tag{a15}$$

This inequality leads to the following quadratic inequality in x:

$$x^2 - \frac{p_2''}{K_H}\left\{\left(\frac{K_H}{p_1''} + \frac{p_1''}{K_H} - 2\right)\frac{3p_1''r}{2\gamma} - \frac{p_1''}{K_H}\right\}x < 0 \tag{a16}$$

By solving this quadratic inequality, the stability condition in eq 8 can be obtained.

A.3. Condition for Constant dr_d/dt

If the dissolution of the PVA aqueous solution into methylene chloride is negligible, the dissolution rate of a spherical methylene chloride droplet into the surrounding PVA aqueous solution, $\dot{m}_1$, can be expressed as follows:

$$\dot{m}_1 = c_1 S_d \frac{dr_d}{dt} \tag{a17}$$

where c_1 is the concentration of methylene chloride inside the droplet and r_d is the radius of the droplet. By using the mass flux of methylene chloride from the surface of a spherical droplet into the surrounding PVA aqueous solution, J_1, $\dot{m}_1$ can also be expressed as follows:

$$\dot{m}_1 = S_d J_1 \tag{a18}$$

where S_d is the surface area of a methylene chloride droplet. From eqs a17 and a18, dr_d/dt can be expressed as follows:

$$\frac{dr_d}{dt} = \frac{J_1}{c_1} \tag{a19}$$

If J_1 is constant, that is, the dissolution rate of methylene chloride is restricted by the surface area of a droplet and is not restricted by the diffusion in the PVA aqueous solution, dr_d/dt remains constant.

References and Notes

(1) Makuta, T.; Takada, S.; Daiguji, H.; Takemura, F. *Mater. Lett.* **2009**, *63*, 703–705.
(2) Stein, M.; Heldmann, D.; Fritzsch, T.; Siegert, J.; Roessling, G. U.S. Patent No. 6,264,959, 2001.
(3) Straub, J. A.; Chikering, D. E.; Church, C. C.; Shah, B.; Hanlon, T.; Bernstein, H. *J. Controlled Release* **2005**, *108*, 21–32.
(4) Wheatley, M. A.; Forsberg, F.; Oum, K.; Ro, R.; El-Sherif, D. *Ultrasonics* **2006**, *44*, 360–367.
(5) Pisani, E.; Tsapis, N.; Paris, J.; Nicolas, V.; Cattel, L.; Fattal, E. *Langmuir* **2006**, *22*, 4397–4402.
(6) Rouzes, C.; Leonard, M.; Durand, A.; Dellacherie, E. *Colloids Surf., B* **2003**, *32*, 125–135.
(7) Bertling, J.; Blömer, J.; Kümmel, R. *Chem. Eng. Technol.* **2004**, *27*, 829–837.
(8) Caruso, F. *Chem.—Eur. J.* **2000**, *6*, 413–419.
(9) Kawahashi, N.; Matijevi, E. J. *J. Colloid Interface Sci.* **1991**, *143*, 103–110.
(10) Strohm, H.; Sgraja, M.; Bertling, J.; Lobmann, P. *J. Mater. Sci.* **2003**, *38*, 1605–1609.
(11) Liu, J. G.; Wilcox, D. L. *J. Mater. Res.* **1995**, *10*, 84–94.
(12) Kaul, S. *Circulation* **1997**, *96*, 3745–3760.
(13) Schutt, E. G.; Klein, D. H.; Mattrey, R. M.; Riess, J. G. *Angew. Chem., Int. Ed.* **2003**, *42*, 3218–3235.
(14) Harris, J. R.; Depoix, F.; Urich, K. *Micron* **1995**, *26*, 103–111.
(15) Daiguji, H.; Makuta, T.; Kinoshita, H.; Oyabu, T.; Takemura, F. *J. Phys. Chem. B* **2007**, *111*, 8879–8884.
(16) Schneider, M. *Eur. Heart J. Suppl.* **2002**, *4* (Suppl. C), C3–C7.
(17) Hoff, L.; Sontum, P. C. *Proc.—IEEE Ultrason. Symp.* **1998**, 1799–1802.
(18) Shchukin, D. G.; Kohler, K; Mohwald, H.; Sukhorukov, G. B. *Angew. Chem., Int. Ed.* **2005**, *44*, 3310–3314.
(19) Ray, S. S.; Bousmina, M. *Prog. Mater. Sci.* **2005**, *50*, 962–1079.
(20) Heino, A.; Naukkarinen, A.; Kulju, T.; Törmälä, P.; Pohjonen, T.; Mäkelä, E. A. *J. Biomed. Mater. Res.* **1996**, *30*, 187–192.
(21) Walovitch, R.; Bernstein, H.; Chickering, D.; Straub, J. U.S. Patent No. 0,271,591, 2005.
(22) Senior, R. *Expert Rev. Cardiovasc. Ther.* **2007**, *5*, 413–421.
(23) Gruber, P. R.; Hall, E. S.; Kolstad, J. J.; Iwen, M. L.; Benson, R. D.; Borchardt, R. L. U.S. Patent No. 5,142,023, 1992.
(24) Narayan, P.; Wheatley, M. A. *Polym. Eng. Sci.* **1999**, *39*, 2242–2255.

(25) Gordillo, J. M.; Cheng, Z.; Ganan-Calvo, A. M.; Marquez, M.; Weitz, D. A. *Phys. Fluids* **2004**, *16*, 2828–2834.

(26) Garstecki, P.; Fuerstman, M. J.; Stone, H. A.; Whitesides, G. M. *Lab Chip* **2006**, *6*, 437–446.

(27) Arakawa, T; Yamamoto, T; Shoji, S. *Sens. Actuators, A* **2008**, *143*, 58–63.

(28) Ward, C. A.; Tikuisis, P.; Venter, R. D. *J. Appl. Phys.* **1982**, *53*, 6076–6084.

(29) Wilhelm, E.; Battino, R.; Wilcock, R. J. *Chem. Rev.* **1977**, *77*, 219–262.

(30) Shirono, K.; Morimatsu, T.; Takemura, F. *J. Chem. Eng. Data* **2008**, *53*, 1867–1871.

(31) Yaw, C. L. *Thermophysical Properties of Chemicals and Hydrocarbons*; William Andrew Publishing: Norwich, NY, 2008.

(32) Perry, R. H.; Green, D. W. *Perry's Chemical Engineers' Handbook*, 7th ed.; McGraw-Hill: New York, 1997.

JP9053956